Sheet superconductivity in WO_{3-x}: crystal structure of the tetragonal matrix

1998 J. Phys.: Condens. Matter 10 L569

(http://iopscience.iop.org/0953-8984/10/33/002)

J. Phys.: Condens. Matter **10** (1998) L569–L574. Printed in the UK PII: S0953-8984(98)95258-4

LETTER TO THE EDITOR

Sheet superconductivity in WO_{3-x}: crystal structure of the tetragonal matrix

A Aird†, M C Domeneghetti‡, F Mazzi‡, V Tazzoli‡ and E K H Salje†

† Department of Earth Sciences, University of Cambridge, Downing Street, Cambridge CB2 3EQ, UK

‡ Consiglio Nazionale Ricerche, C S Cristallochimica e Cristallografia, c/o Dipartimento di Scienze della Terra, Università di Pavia, Via Ferrata 1, 27100 Pavia, Italy

Received 22 June 1998

Abstract. Sheet conductivity was found in oxygen reduced WO_{3-x}. The sheets are aligned along the twin boundaries of the unreduced starting material (β-WO_3). The bulk transforms during the oxygen loss to a WO_{3-x} phase with tetragonal crystal structure. The space group is $P\bar{4}2_1m$ with lattice parameters $a = 0.739$ nm and $c = 0.388$ nm. The perovskite-like structure contains distorted octahedra with W–O distances between 0.17 nm and 0.218 nm.

Sheet superconductivity in WO_{3-x} single crystals was discovered by Aird and Salje [1]. The crystals were produced by chemical reduction of WO_3 using Na-vapour as reducing agent. Chemical analysis showed that oxygen was removed from the sample while no sodium was incorporated into the reaction product.

Crystals of WO_3 with twin boundaries were reduced inhomogeneously with higher degrees of reduction along the twin boundaries. These highly reduced sheets were found to be superconducting while no superconductivity was observed in the bulk of the crystal. The reduction of a single crystal of WO_3 leads to a single crystal of WO_{3-x}. Two transformations occur during reduction: firstly the twin boundaries are transformed into superconducting sheets, and, secondly, the bulk of the material undergoes a structural transformation to a novel crystal structure of WO_{3-x}. It is the purpose of this letter to describe this new structure.

Fully oxidized WO_3 crystallizes in a perovskite-type structure. It undergoes four structural phase transitions under heating and cooling with the known structures:

α: tetragonal at 770 °C [2, 3]
$a = 0.5250$ nm $c = 0.3915$ nm
β: orthorhombic at 480 °C [3]
$a = 0.7341$ nm $b = 0.7570$ nm $c = 0.7754$ nm
γ: monoclinic at room temperature [4]
$a = 0.7306$ nm $b = 0.7540$ nm $c = 0.7692$ nm $\beta = 90.88°$
δ: triclinic at room temperature [5, 6]
$a = 0.7309$ nm $b = 0.75165$ nm $c = 0.76811$ nm $\alpha = 88.81°$ $\beta = 90.985°$
$\gamma = 90.985°$
ε: monoclinic at 10 K [6]
$a = 0.52771$ nm $b = 0.71555$ nm $c = 0.76630$ nm $\beta = 91.76°$

0953-8984/98/330569+06$19.50

Most oxygen deficient WO_{3-x} crystallizes into phases containing crystallographic shear (CS) planes in various directions [7, 8] or pentagonal tunnel structures [9]. First x-ray diffraction experiments on the new WO_{3-x} material showed no indication of CS or tunnel structure while subsequent grinding of the single crystals leads to small crystallites which were riddled with CS planes. Transmission electron microscope observations showed that the CS planes were of the {102} type [10].

The WO_3 samples were made by recrystallizing WO_3 powder to small single crystals, as described by Salje and Viswanathan and Locherer *et al* [11, 12]. To reduce the WO_3 samples, WO_3 and Na metal are placed in opposite ends of a sealed evacuated U-shaped silica tube, and heated to 730 K for varying amounts of time. The Na vapour is transported to the WO_3 and reduces the surface while forming Na_2O. The high oxygen mobility within the sample results in subsequent reduction of the sample further from the surface.

The reduced sample changes colour from yellow–green to an opaque dark blue. A range of samples were measured for resistivity at low temperature using a standard 4-probe technique, and by SQUID magnetometer to test for superconductivity. Several samples were found to have filamentary superconductivity but not bulk [1]. One of these samples, reduced for 6 hours, was selected, and single-crystal diffraction was used to find the structure of the bulk material. The low-temperature resistance measurements indicate that our sample is very close to the Anderson transition at $WO_{2.90}$ [13] but not yet metallic. Hence we expect x to be slightly less than 0.1 in the superconducting phase and the bulk to be even less than that, probably around $WO_{2.95}$.

X-ray diffraction intensity data were collected on an optically selected single crystal of WO_{3-x} using a Philips PW1100 four-circle automated diffractometer and graphite monochromatized MoKα radiation ($\lambda = 0.71073$ Å). Operating conditions were 60 kV and 25 mA. Horizontal and vertical detector apertures were 2.0° and 1.5° respectively. Net x-ray diffraction intensities were obtained by measuring step-scan profiles and analysing them by the Lehmann and Larsen [14] σ_I/I method, as modified by Blessing *et al* [15]. All sixteen equivalent reflections in Laue symmetry class $4/mmm$ were measured. Three standard reflections were measured every two hundred reflections. Unit cell parameters were determined by centring 57 reflections, using a locally improved version [16] of the Philips LAT routine, and are reported in table 1 together with other experimental details. Intensities were corrected for absorption using the semi-empirical method of North *et al* [17] and the values of the equivalent reflections were averaged; the resulting discrepancy factor R_{sym} is reported in table 1.

A preliminary examination of the symmetry of reflections and of the systematic extinctions suggested two possible non-centric space groups $P42_12$ and $P\bar{4}2_1m$. The absence of the symmetry centre was confirmed by the statistical analysis of structure factor amplitudes [18]. The structure was solved in the space group $P\bar{4}2_1m$, while an attempt in $P42_12$ was unsuccessful. The structure refinement was done without chemical constraints, using a locally modified version of the least-square program ORFLS [19]. There were 203 reflections, with $I > 3\sigma I$, considered to be observed and used for the refinement with unit weights. The atomic scattering curve for neutral W and O were taken from the International Tables for X-ray Crystallography [20]. The extinction correction by [21] was applied. Isotropic displacement parameters were used in the first cycles of refinement and anisotropic displacement parameters for all atoms in the final cycles, varying all parameters simultaneously together with scale factor and extinction coefficient. No correlation between variables greater than 0.77 was observed. The refinement converged to a residual index R_{obs} of 3.22% for the observed reflections and R_{all} of 3.85% for all measured reflections. The final difference-Fourier map was featureless. The final atomic parameters are given

Table 1. X-ray crystal and refinement data.

a (nm)	0.739(2)
c (nm)	0.388(1)
Unit cell volume (nm^3)	0.2119
Space group	$P\bar{4}2_1m$
Crystal dimensions (mm)	$0.06 \times 0.07 \times 0.26$
Radiation	MoKα
Scan mode	ω
Scan width (°)	3.00
θ range (°)	2–30
Measured reflections ($\pm h \pm k \pm l$)	2510
Unique reflections	223
Observed reflections[a]	203
R_{sym}[b]	4.92%
R_{obs}[c]	3.22%
R_{all}[c]	3.85%

[a] Only the reflections with $I \geqslant 3\sigma(I)$ were considered as observed.
[b] $R_{sym} = \sum_{hkl} \sum_{i=1}^{N} |F_0^2(hkl)_i - \bar{F}_0^2(hkl)| / \sum_{hkl} \sum_{i=1}^{N} F_0^2(hkl)_i$ where $F_0^2(hkl)_i$ refers to the ith equivalent of the reflection hkl and $\bar{F}_0^2(hkl)$ is the mean value of the N equivalent reflections.
[c] R_{obs} and R_{all} are the final descrepancy indicies expressed as $\sum ||F_0| - |F_c|| / \sum F_0$.

Table 2. Atomic positional and equivalent isotropic displacement parameters. Numbers in parentheses are the ESDs. Atomic positional parameters of tetragonal WO_3 phase, recalculated within the unit cell of WO_{3-x}, are reported in brackets for comparison.

Atom	x/a	y/b	z/c	U_{eq}
W	0.2569(1)	0.7569(1)	−0.0698(2)	0.0183(2)
	[0.25]	[0.75]	[−0.0768]	
O^1	0.2633(40)	0.7633(40)	0.4930(50)	0.0697(70)
	[0.25]	[0.75]	[0.4865]	
O^2	0.0021(22)	0.7915(22)	0.0241(47)	0.0418(58)
	[0.0]	[0.75]	[0.0]	

Table 3. Anisotropic displacement parameters. Numbers in parentheses are the ESDs.

Atom	U_{11}	U_{22}	U_{33}	U_{12}	U_{13}	U_{23}
W	0.0209(3)	0.0209(3)	0.0129(4)	0.0001(8)	0.0004(3)	0.0004(3)
O^1	0.0970(142)	0.0970(142)	0.0150(64)	0.0384(342)	0.0052(94)	0.0052(94)
O^2	0.0304(68)	0.0452(144)	0.0497(74)	0.0045(70)	−0.0018(80)	0.0089(102)

in tables 2 and 3, bond distances and angles are listed in table 4. A list of observed and calculated structure factors may be obtained on request from the authors. Figure 1 shows a picture of the structure.

The WO_{3-x} sample has a structure similar to that of the high-temperature α phase of unreduced WO_3, which has recently been described within the space group $P4/nmm$, with unit cell parameters $a = 0.52916$ nm and $c = 0.39255$ nm, $V = 0.1099$ nm^3 [22]. However, because of the superlattice reflections which have been observed by x-ray single-crystal diffraction, the unit cell volume of WO_{3-x} phase turned out to be twice that of unreduced WO_3, with $a = 0.739$ nm (close to $a_{WO_3}\sqrt{2}$) and $c = 0.388$ nm, $V = 0.2119$ nm^3. Figure 2

Table 4. Bond distances (nm) and angles (°). Numbers in parentheses are the ESDs.

W–O^1	0.218(2)	O^1–W–O^1	176(1)
W–O^1	0.170(2)	O^1–W–O^2	80(1) × 2
W–O^2	0.194(2) × 2	O^1–W–O^2	84(1) × 2
W–O^2	0.186(2) × 2	O^1–W–O^2	102(1) × 2
		O^1–W–O^2	94(1) × 2
Mean	0.191	O^2–W–O^2	70(1) × 2
OQE[a]	0.106	O^2–W–O^2	163(1) × 2
		O^2–W–O^2	103(1)
		O^2–W–O^2	112(1)

[a] Octahedral quadratic elongation (Robinson *et al* 1971).

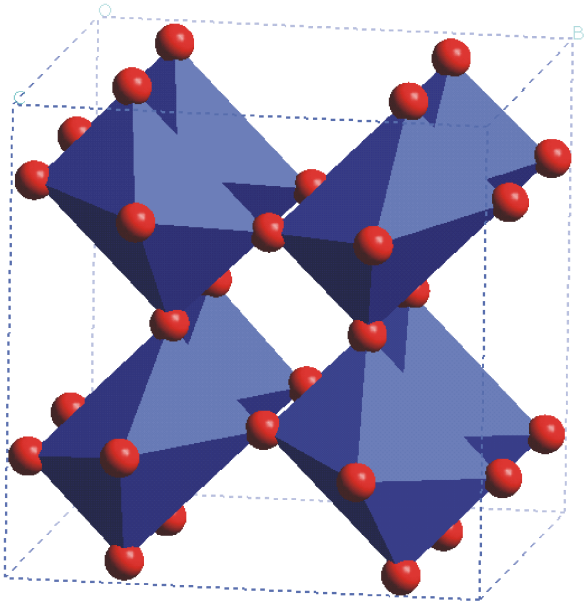

Figure 1. Crystal structure of tetragonal WO_{3-x}.

shows the relationship between the two unit cells. The atomic positions of the two phases are very close, as is evident from table 2 which compares the values of the atomic positions of WO_{3-x} with those of WO_3, recalculated within the unit cell of WO_{3-x}. The largest shifts concern oxygen O^2 and their directions are indicated in figure 2. The high values of U_{eq} of the two oxygens O^1 and O^2 could be ascribed to an incomplete site occupancy or to a partial disorder distribution. Attempts were made to locate any sodium in the structure, but the differences-Fourier map did not give any evidence for its presence. Repeated microprobe analysis confirmed the result that no sodium was incorporated into the crystal structure.

The structure analysis showed that the samples were crystals with no visible diffraction signal from the vanishingly small volume part of the superconductivity sheets. The domains adjacent to these sheets were twin related in the unreduced starting material with a spontaneous rotation of 0.88° [12]. The twin orientations at room temperature are to the ferroelastic twin planes of the α–β and β–γ transitions [23]. The orientation of the

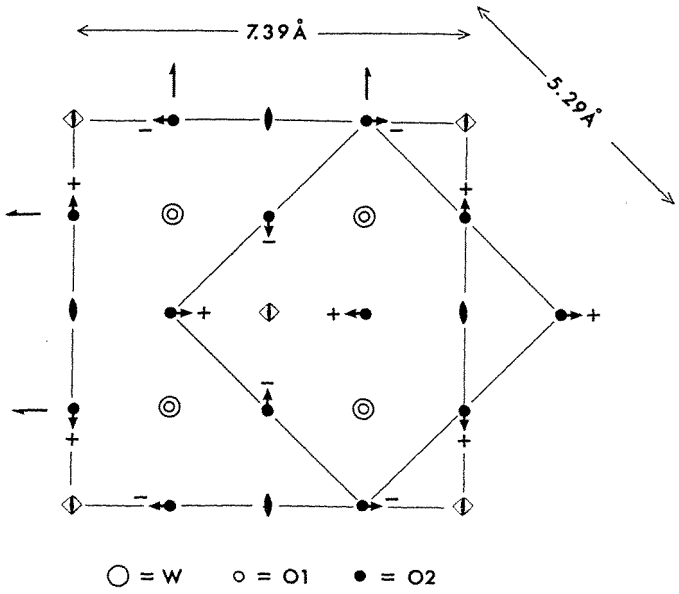

Figure 2. Relationship between the unit cell of unreduced WO_3 (space group $P4/nmm$) and that of reduced WO_{3-x} (space group $P\bar{4}2_1m$). Symmetry elements of space group $P\bar{4}2_1m$ (except mirror and slide planes) are reported. Arrows indicate the shift of the position of each O^2 oxygen in the (001) plane from the WO_3 to the WO_{3-x} structure. Symbols + and − indicate the direction of the shift along the c axis.

tetragonal structure is such that no twinning remains in the reduced sample. The orientation of the tetragonal cell is then determined by its common c axis with the α and β structures. Its crystallographic a and b axis are parallel to the corresponding axes of the orthorhombic β phase and rotated by 45° against the planes of the superconducting sheets.

The observation that the bulk material has transformed uniformly leaves the superconducting sheets as confined structural units with, at present, unknown atomic structure. It shows that confinement of superconductivity to such sheets is physically possible and leads to a multitude of options for device applications on a true nanometre scale. From a purely scientific perspective it may open the door for a novel way to investigate correlation effects, superconducting weak links, Andreev mirrors, vortex motions in such sheets and so forth [24–26]. Attempts are being made to further investigate the nature of the superconducting sheets.

We are grateful to Kim Locherer for preparing the unreacted WO_3 crystals, and for helpful discussions. Thanks to Michele Warren for assistance in generating figure 1.

References

[1] Aird A and Salje E K H 1998 *J. Phys. Condens. Matter* **10** L377–80
[2] Kehl W L, Hay R G and Wahl D 1952 *J. Appl. Phys.* **23** 212
[3] Salje E 1977 *Acta Crystallogr.* B **33** 574
[4] Woodward P M and Sleight A W 1997 *J. Solid State Chem.* **131** 9
[5] Diehl R, Brandt G and Salje E 1978 *Acta Crystallogr.* B **24** 1105
[6] Salje E K H, Rehmann S, Pobell I, Morris D, Knight K S, Herrmannsdörfer T and Dove M T 1997 *J. Phys.: Condens. Matter* **9** 6563

[7] Ekström T, Salje E and Tilley R J D 1981 *J. Solid State Chem*. **40** 75
[8] Salje E, Gehlig R and Viswanathan K 1978 *J. Solid State Chem.* **25** 239
[9] Viswanathan K, Brandt K and Salje E 1981 *J. Solid State Chem.* **36** 45
[10] Sundberg M 1980 *J. Solid State Chem.* **35** 120
[11] Salje E and Viswanathan K 1975 *Acta Crystallogr*. A **31** 356
[12] Locherer K R, Chrosch J and Salje E K H 1998 *Phase Transitions* to be published
[13] Salje E and Güttler B 1984 *Phil. Mag.* **350** 607
[14] Lehmann M S and Larsen F K 1974 *Acta Crystallogr*. A **30** 580
[15] Blessing R H, Coppens P and Becker P 1974 *J. Appl. Crystallogr.* **7** 488
[16] Cannillo E, Germani G and Mazzi F 1983 New crystallographic software for Philips PW 1100 single crystal diffractometer *Internal Report 2* CNR Centro di Studio per la Cristallografia
[17] North A C T, Phillips D C and Mathews F S 1968 *Acta Crystallogr*. A **24** 351
[18] Howells E R, Phillips D C and Rogers D 1950 *Acta Crysallogr*. **3** 210
[19] Busing W R, Martin K O and Levy H S 1962 *ORFLS, A Fortran Crystallographic Least-squares Program* US National Technical Information Service, ORNL-TM 305
[20] Ibers J A and Hamilton W C (ed) 1974 *International Tables for X-ray Crystallography* vol 4 (Birmingham: Kynoch) pp 99–101
[21] Coppens P and Hamilton W C 1970 *Acta Crystallogr*. A **26** 71
[22] Locherer K and Salje E K H 1998 in preparation
[23] Salje E K H 1993 *Phase Transitions in Ferroelastic and Co-elastic Crystals* (Cambridge: Cambridge University Press)
[24] Imry Y 1997 *Introduction to Mesoscopic Physics* (Oxford: Oxford University Press)
[25] Furusaki A *et al* 1991 *Solid State Commun.* **78** 290
[26] Furusaki A, Takayangi H and Tsukada M 1991 *Phys. Rev. Lett.* **67** 132